

REPORT



Decoding the mannose receptor-mAb interaction: the importance of high-mannose N-glycans and glycan-pairing

Julia Baumeister^{a,b}, Maximilian Meudt^{a,c}, Sybille Ebert^d, Frank Rosenau^b, Boris Mizaikoff^c, Michaela Blech^a, Kristina M. J. Aertker^a, and Fabian Higel^e

^aAnalytical Development Biologicals, Boehringer Ingelheim Pharma GmbH & Co. KG, Biberach an der Riss, Germany; ^bInstitute of Pharmaceutical Biotechnology, Ulm University, Ulm, Germany; ^cInstitute of Analytical and Bioanalytical Chemistry, Ulm University, Ulm, Germany; ^dInstitute of Applied Biotechnology, Biberach University of Applied Sciences, Biberach an der Riss, Germany; ^eGlobal CMC Experts NBE, Boehringer Ingelheim Pharma GmbH & Co. KG, Biberach an der Riss, Germany

ABSTRACT

During the development process of therapeutic monoclonal antibodies (mAbs), it is crucial to control (critical) quality attributes such as N-glycosylation influencing pharmacokinetics (PK) and Fc effector functions. Previous reports have shown that mAbs containing high-mannose N-glycans are cleared faster from blood circulation, leading to reduced half-lives. The high-mannose N-glycan content of mAbs can be influenced during the cell culture process by factors such as cell lines, process conditions, and media. Furthermore, mAbs have either one high mannose N-glycan (asymmetrical high-mannose glyco-pair) or two high mannose N-glycans (symmetrical high-mannose glyco-pair). The hypothesis that the mannose receptor (MR, CD206) accelerates clearance by facilitating their internalization and subsequent lysosomal degradation is widespread. However, the interaction between MR and mAbs has not been explicitly demonstrated. This study aimed to investigate this interaction, providing the first systematic demonstration of MR binding to the Fc region of mAbs with high-mannose N-glycans. Two novel analytical methods, MR surface plasmon resonance and MR affinity chromatography, were developed and applied to investigate the MR-mAb interaction. The interaction is found to be dependent on high-mannose content, but is independent of the mAb format or sequence. However, different glyco-pairs exhibited varying binding affinities to the MR, with the symmetrical high-mannose glyco-pair showing the strongest binding properties. These findings strengthen the hypothesis for the MR-mediated mAb interaction and contribute to a deeper understanding of the MR-mAb interaction, which could affect the criticality of high-mannose containing mAbs development strategies of IgG-based molecules and improve their PK profiles.

ARTICLE HISTORY

Received 27 May 2024
Revised 29 August 2024
Accepted 30 August 2024

KEYWORDS

N-glycosylation;
high-mannose;
glycan-pairing; mannose
receptor; monoclonal
antibody; pharmacokinetics;
SPR; affinity chromatography

Introduction


The pharmacokinetics (PK) of therapeutic monoclonal antibodies (mAbs), such as the clearance rate and half-life, are crucial for their efficacy as drug candidates and are influenced by several factors. The neonatal Fc receptor (FcRn) is known to regulate the serum half-life of mAbs, a process that is hardly affected by the N-glycans of mAbs. However, other receptors, such as the asialoglycoprotein receptor and the mannose receptor (MR), can facilitate the clearance of mAbs dependent on specific N-glycans.¹ Early studies² indicated that administration of yeast mannan slows down the clearance of IgG1-Lec1, a mAb with high-mannose N-glycans. This suggests the involvement of a mannose-specific lectin, i.e., the MR, in the clearance mechanism. Furthermore the MR is involved in the faster clearance of high-mannose-containing glycoproteins like ovalbumin, bovine serum albumin (BSA), tissue plasminogen activator (TPA) or a mannosylated antibody-enzyme fusion protein.^{3–6}

The MR plays a crucial role as an endocytic and phagocytic pattern recognition receptor in the immune system. The MR

binds in a calcium-dependent manner to specific carbohydrate structures, such as high-mannose, fucose or N-acetylglucosamine N-glycans, on the surface of various pathogens and endogenous glycoproteins.^{7,8} This interaction facilitates the clearance of these molecules from circulation and contributes to the regulation of immune responses.⁹ The MR is predominantly expressed on the surface of macrophages (e.g., Kupffer cells), dendritic cells, and certain endothelial cells. Structurally, the MR is a type I transmembrane glycoprotein, and its extracellular region is composed of a N-terminal cysteine-rich domain, a fibronectin type II domain, and eight C-type lectin-like domains (CTLDs). CTLD4, along with CTLD5, is primarily responsible for binding to high-mannose structures on glycoproteins. Hence, these two domains are typically referred to as carbohydrate recognition domains (CRDs) 4 and 5.^{8,10–12} The homeostasis mechanism of endogenous glycoproteins reveals that the MR has the ability to internalize glycoproteins.^{5,7}

Recent findings have shed light on the faster clearance of therapeutic mAbs containing high-mannose N-glycans in

CONTACT Fabian Higel  fabian.higel@boehringer-ingelheim.com  Global CMC Experts NBE, Boehringer Ingelheim Pharma GmbH & Co. KG, Birkendorfer Strasse 65, Biberach an der Riss 88397, Germany

 Supplemental data for this article can be accessed online at <https://doi.org/10.1080/19420862.2024.2400414>

© 2024 Boehringer Ingelheim. Published with license by Taylor & Francis Group, LLC.

This is an Open Access article distributed under the terms of the Creative Commons Attribution-NonCommercial License (<http://creativecommons.org/licenses/by-nc/4.0/>), which permits unrestricted non-commercial use, distribution, and reproduction in any medium, provided the original work is properly cited. The terms on which this article has been published allow the posting of the Accepted Manuscript in a repository by the author(s) or with their consent.

different organisms. It has been observed that the relative level decrease for high-mannose N-glycans is a function of circulation time, while other complex N-glycans remain constant. The recent PK data indicate an effect of the N-glycan and not of the protein itself.^{2,13–18} It is believed that glycosidases in circulation convert high-mannose structures from M6–M9 into the smaller structure, M5.¹⁹ Notably, this *in vivo* enzymatic conversion from M6–M9 to M5 results in a temporary increase of M5 within the first hours after administration. However, due to enzyme specificity, this mechanism does not extend to M5, necessitating a separate explanation for its faster clearance.^{13,16,17,20} While the half-life of serum IgG is typically mediated by FcRn, differences in FcRn binding could potentially be the reason for the variance in clearance among glycoforms.²¹ Nevertheless, the impact of post-translational modifications is largely defined by oxidation of Met252 in the Fc region of mAbs and the different glycoforms lead only to minor differences in FcRn binding, which are unlikely to translate into a PK difference *in vivo*.^{22–25} The findings corroborated the theory that a receptor possessing lectin-like characteristics, like the MR, is necessary for the faster clearance of high-mannose containing mAbs. A more plausible reason for the preferential clearance of certain mAbs containing high-mannose N-glycans could be the clearance process facilitated by naturally present lectins on mammalian cell surfaces. A hypothesis suggesting that the MR contributes to the faster clearance of high-mannose-containing mAbs has been proposed.^{2,13–17}

mAbs, based on IgG1, are glycoproteins with one N-glycosylation site at each heavy chain (Asn297 (EU numbering)), leading to a combination of two N-glycans, hereinafter assigned to glyco-pair.^{26–28} There are three types of N-glycans: complex, hybrid or high-mannose type structures.²⁹ Recombinant mAbs produced in Chinese hamster ovary (CHO) cells primarily contain complex N-glycans, in detail biantennary fucosylated neutral glycans with varying levels of terminal galactose, along with some high-mannose structures. High-mannose N-glycans were recently reported to average between less than 1% to 3%.³⁰ However, the high-mannose content can be up to 25–35% due to factors in the cell culture process, such as cell line, process conditions and media compositions.^{31–33} Furthermore, mAbs can include either one high-mannose N-glycan (asymmetrical high-mannose glyco-pair) or two high-mannose N-glycans (symmetrical high-mannose glyco-pair).³⁴

This knowledge may help to explain the clearance mechanism of therapeutic mAbs containing high-mannose N-glycans. Based on it, the following hypothetical MR-mediated clearance process could be proposed. With the binding of the mAbs to the MR at the cell surface under physiological conditions (pH 7.4, in the presence of Ca²⁺), an MR-mAb complex is formed. The complex is then internalized into the cell. In the cell endosome, a pH-dependent conformational change of the MR through acidification results in the disruption of the MR-mAb interaction. The mAbs are finally degraded in the lysosome, while the MR is then recycled back to the cell surface.^{5,8,35–37} The reason why the high-mannose containing mAb is not immediately rescued in the endosome via the FcRn salvage pathway, despite the co-expression of FcRn and MR in a variety of cells, has not been investigated. This could

potentially be attributed to the presence of endogenous IgGs in the late endosome, which are nonspecifically internalized and compete with the therapeutic mAbs for binding to FcRn. If the concentration of endogenous IgGs is sufficiently high, they will be rescued first, likely leading to the degradation of the high-mannose-containing mAbs. However, this hypothesis cannot be explained by available data and is not the subject of this study.

The binding mechanism of the MR to mAbs has not been systematically shown, which could lead to potential inaccuracies in critical quality attribute (CQA) assessments. The aim of this study was to gain a deeper understanding of the MR-mAb interaction to strengthen the hypothesis, which will inform development strategies of IgG-based molecules and contribute to the ongoing efforts to improve their PK profiles. This study provides insights into the interaction of therapeutic mAbs with the MR, as well as factors influencing the interaction, such as high-mannose N-glycan content, mAb design and format, and symmetrical or asymmetrical high-mannose glyco-pairs. Novel analytical methods have been developed and applied, including mannose receptor-surface plasmon resonance (MR-SPR) analysis and mannose receptor-affinity chromatography (MR-AC) to investigate the MR-mAb interaction.

Results

mAbs with different high-mannose content

In this study, the MR interaction with 11 mAbs, including different IgG based formats such as IgG1 and IgG4, as well as bispecific formats, was investigated. The starting material of these mAbs (reference mAb) revealed a typical IgG N-glycosylation profile as characterized by glycan map. The N-glycans were primarily composed of A2G0F and A2G1F, and 2–16% high-mannose N-glycans, mainly M5, as exemplarily demonstrated for IgG1-A (Figure 1a). In order to more sensitively examine the MR-mAb interaction, two approaches were used to produce material with a higher high-mannose content. First, material with enriched high-mannose N-glycan content was prepared by Concanavalin A (ConA) chromatography. ConA chromatography is a type of lectin affinity chromatography that selectively binds to alpha-mannose moieties.³⁸ In a second approach to produce material with predominantly high-mannose N-glycans, specifically M5–M9, kifunensine, a mannosidase inhibitor, was used in the cell culture process.^{20,39} The high-mannose content of all materials was quantified by glycan map. The glycan map profiles comparing the reference mAb with the respective ConA product pool and the material expressed with kifunensine, are presented using IgG1-A as an example (Figure 1a,b,c). As a result, the ConA product pool of the 11 mAbs was enriched in high-mannose N-glycans to a range of 35–56% and the kifunensine material contained 87–96% high-mannose N-glycans. Along the observed enrichment of high-mannose N-glycans in the ConA product pool, there was an increase in truncated, mono-antennary complex N-glycans, indicating preferred pairing with high-mannose N-glycans. The relevant N-glycan structures are presented in Figure S1.

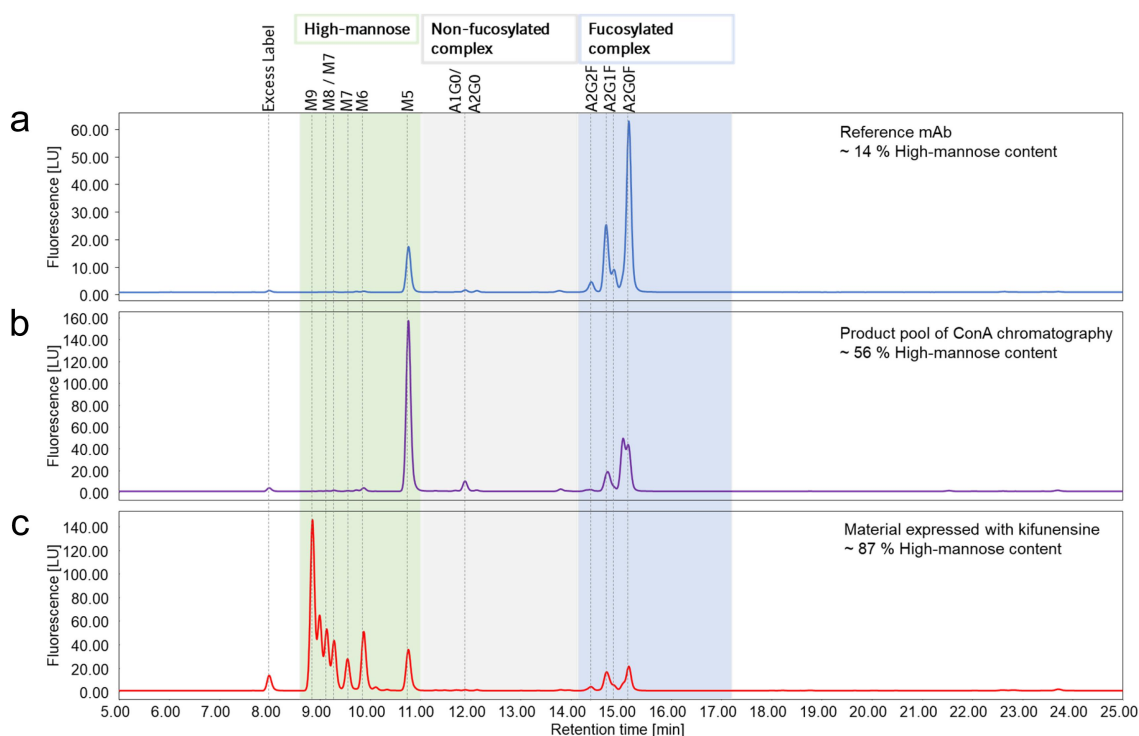


Figure 1. Overview of the glycan map chromatograms of the material with different high-mannose content. The reference mAb (a), which was also enriched in high-mannose content by ConA chromatography (b) and expressed with kifunensine (c) is shown exemplified for IgG1-A. The main N-glycan structures are annotated to their respective peaks.

Analytical methods to investigate MR – mAb interaction

Two distinct orthogonal methods were developed to investigate the interaction between the MR and mAbs: MR-SPR analysis with the full-length extracellular domain of MR immobilized on the sensor chip and MR-AC, which uses the full-length extracellular domain of MR coupled to the resin. The MR was produced in transiently transfected HEK-F cells and was subsequently purified to $\geq 95\%$ monomer. RNase B, a high-mannose glycoprotein with a single N-glycosylation site⁴⁰ containing mainly M5 and M6 N-glycans (Table S1), was used to set up the methods.

Given that MR interacts with other glycoproteins in a Ca^{2+} -dependent manner under physiological pH of 7.4,^{8,37} RNase B binding to MR was explored whether it is influenced by pH and Ca^{2+} . For MR-SPR analysis, the association and dissociation of the RNase B was measured. RNase B binds to MR under physiological pH of 7.4 in presence of Ca^{2+} , but did not bind under physiological conditions in absence of Ca^{2+} and at acidic environment (pH 5.0) in presence of Ca^{2+} mimicking endosomal conditions (Figure S2a). For MR-AC, the binding conditions were evaluated in different steps using RNase B. The binding of mAbs to the MR was achieved under physiological-like conditions, requiring pH 7.4 with Ca^{2+} , whereas binding conditions at pH 7.4 without Ca^{2+} or at pH 5.0 with Ca^{2+} showed no interaction. In the following steps, the chromatographic elution conditions were optimized by testing both a pH gradient and an ethylenediaminetetraacetic acid (EDTA) gradient. It has been reported that the acidification and the lower concentration of Ca^{2+} in the endosomes are essential for the ligand-receptor dissociation.³⁵ While the pH gradient did not lead to an elution peak of RNase B, the EDTA

gradient achieved the desired elution peak. The injection of RNase B onto the column revealed a single peak at 14.0 min retention time and 20.7% elution buffer B corresponding to ~ 4.1 mM EDTA (Figure S2b). Furthermore, the specificity of the column was tested using BSA. The injection of BSA onto the column revealed a flow-through peak at 1.9 min (0%B) (Figure S2c).

Binding of MR to IgGs dependent on high-mannose N-glycans and regardless of mAb format or sequence

To investigate if mAbs bind to the MR and the interaction is dependent on high-mannose N-glycans, IgG1-A and IgG4 with varying high-mannose content were analyzed using MR-SPR. IgG1-A comprised between 14% and 87% high-mannose content and IgG4 contained between 2% and 96% high-mannose content. Deglycosylated mAbs were used as controls. For deglycosylation, IgG1-A and IgG4 were treated with Endo S, which removed all N-glycans with or without core fucosylation, except for the initial N-acetylglucosamine residue. This complete deglycosylation of the mAbs was confirmed by reverse phase chromatography (RPC) - mass spectrometry (MS) and hydrophilic interaction liquid chromatography (HILIC) (Figure S3). The MR-SPR analysis showed an enhanced response signal with higher high-mannose content for both mAbs. No binding of EndoS treated IgG1-A and IgG4 was detected (Figure 2a,b).

To examine if M9 to M6 N-glycans exhibit a different binding response than M5 N-glycans, the IgG1-A with 87% M9 to M5 N-glycans were digested with α -1,2-mannosidase to obtain IgG1-A with primarily M5 N-glycans. The digestion

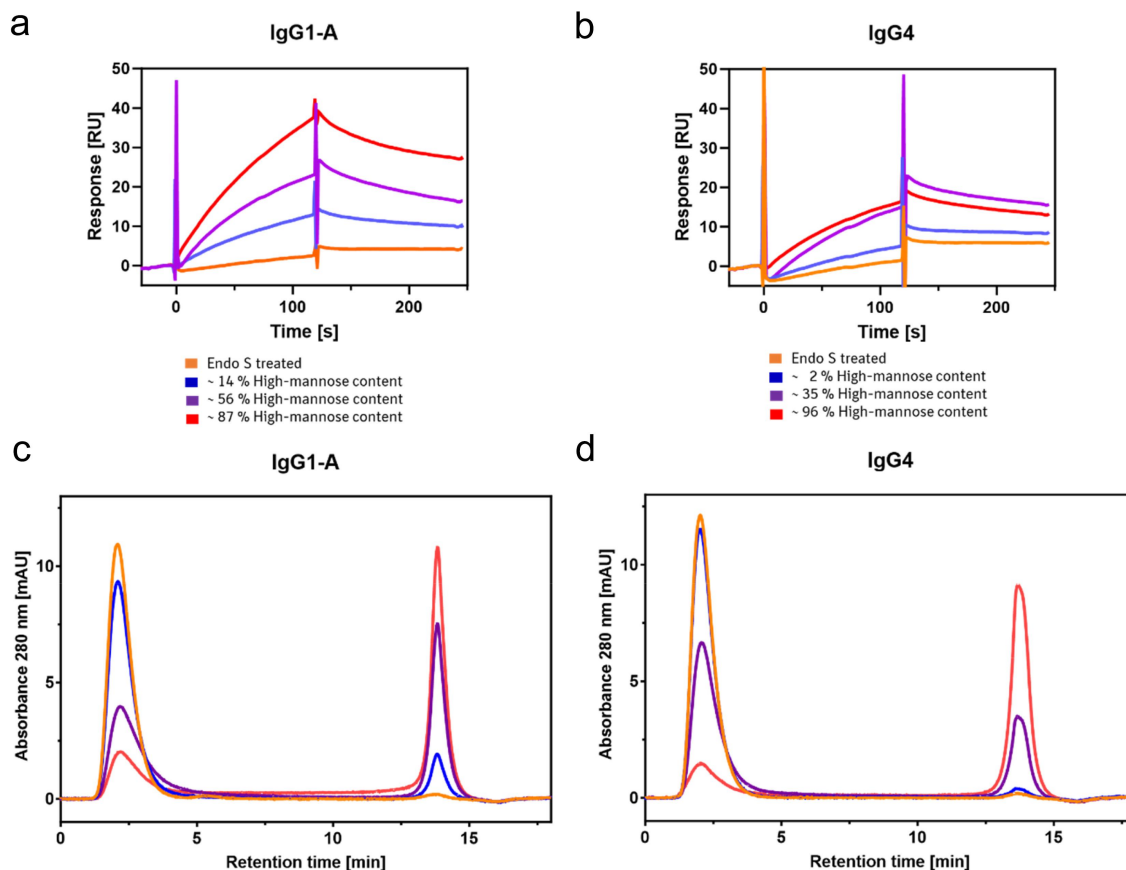


Figure 2. Interaction of IgG1-A (a,c) and IgG4 (b,d) with the MR analyzed by MR-SPR. Different high-mannose variants of each mAb are compared to the Endo S treated control, reflecting a deglycosylated mAb.

was monitored by intact RPC-MS (Figure S4a). The MR-SPR results showed high similarity in association and complex dissociation between IgG1-A with M5 and IgG1-A with M9 to M5 (Figure S4b).

To examine the impact of other factors than high-mannose content on MR binding, such as mAb format or sequence, characterization of the binding between the MR and RNase B or six mAbs was conducted using MR-SPR analysis. These reference mAbs, which vary in their sequences and formats, included IgG1 and bispecific formats known as ZweimAb (two chain knob-into-hole construct) or DoppelmAb (IgG1-scFv), which have been previously described⁴¹ and are schematically illustrated in Figure 3c. The sequence and structure of the IgG1-based Fcs, especially the carbohydrate-containing C_H2 domain, is identical among the tested molecules except for substitutions for the knob-into-hole construct or effector function silencing substitutions.

Varying concentrations of RNase B and the mAbs were injected onto the SPR sensor chip surface and binding responses were recorded and analyzed. Figure S5 shows the representative datasets obtained from the analysis of MR-

RNase B and MR-mAb interactions with steady state affinity analyses. From the data set, apparent binding affinity constants (K_D) were obtained. K_D values were all in the single-digit μ M range (2.7–6.3 μ M), demonstrating that all constructs bind with similar affinity via their N-glycans to the MR independent of their differences in format or sequence. Only RNase B showed a slightly different binding behavior ($K_D = 1.3 \mu$ M) (Table 1).

MR-SPR analysis was chosen to provide overall kinetic or binding data of the MR-mAb interaction. MR-AC was applied as a low-pressure functional chromatography orthogonal to MR-SPR to further characterize the MR-mAb interaction and reflect or resolve mAb heterogeneity regarding the various N-glycan structures. The MR-AC method was set up in a bind-elute mode that separated mAb variants due to different bindings affinities in the flow-through peak or/and elution peak. Optional fractionation and secondary analysis facilitated the identification of the variants. Investigations were conducted to compare the results of MR-SPR by MR-AC analysis of IgG1-A and IgG4 high-mannose and deglycosylated variants. The analysis by MR-AC was evaluated by determining the elution peak

Table 1. Measured K_D values of MR interaction for different mAbs and RNase B by MR-SPR. Data are shown as mean of 4-fold measurement for RNase B and duplicate measurement for mAbs. The mean K_D value of all six mAbs was calculated.

Molecule	RNase B	IgG1-A	IgG1-B	IgG1-C	ZweimAb-A	ZweimAb-B	DoppelmAb-B	Mean mAbs
K_D [$\ast 10^{-6}$ M]	1.3	4.1	5.4	4.5	3.7	2.7	6.3	4.5 ± 1.3

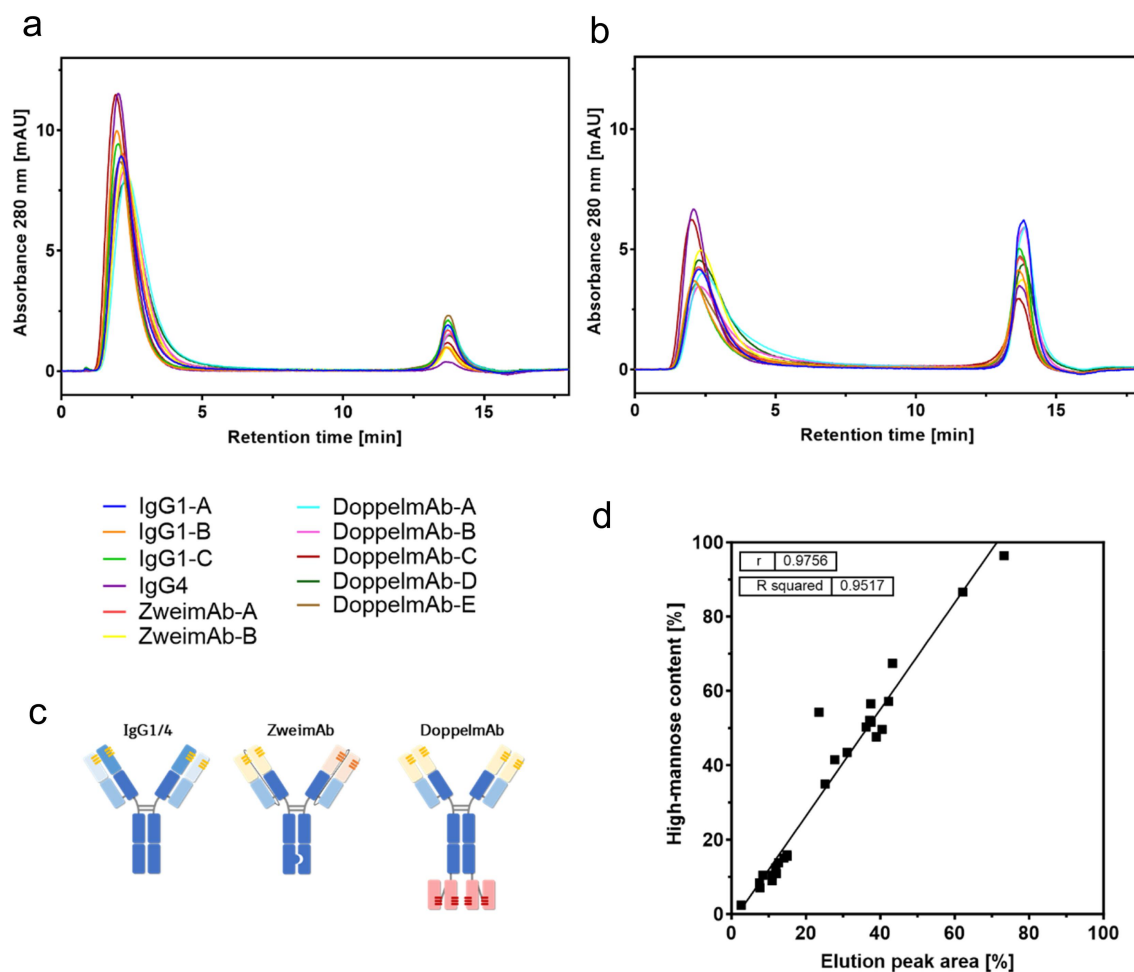


Figure 3. MR-AC analysis of mAbs differing in their sequence and format. The chromatograms of the reference mAbs (a) and the ConA product pools (b) of 11 different mAbs are overlaid. The schematic illustration of the different formats is shown (c). The elution peak areas of the MR-AC analysis are correlated with the respective high-mannose content of the mAbs (d).

area reflecting MR binding. For both mAbs, the elution peak area increased with increasing high-mannose content, and all mAbs eluted with the same retention time at 13.8 min. An increase in high-mannose content led to a decrease in the flow-through peak area. Additionally, an increase in high-mannose content resulted in more noticeable asymmetry of the flow-through peak due to tailing suggesting a slight MR interaction. Endo S treated IgG1 A and IgG4 eluted in the flow-through demonstrating no observable MR binding (Figure 2c,d). A panel of 11 mAbs was screened to compare the elution peak area obtained from the MR-AC with the high-mannose content as determined by glycan map. This was done for both the reference mAbs and the ConA product pools (Figure 3a,b). The elution peaks of all mAbs exhibited identical retention times, with differences only in elution peak area. The flow-through peak, however, displayed differences in peak shape, with more pronounced tailing observed for the ConA product pools. The results demonstrated a linear correlation between the elution peak area of the MR-AC and the high-mannose content of the glycan map (Figure 3d). Overall, this indicates that the high-mannose N-glycan of the Fc primarily contributes to the MR binding.

Avidity effect for symmetrical high-mannose glyco-pair of mAbs with MR

Due to the pronounced peak tailing of the flow-through peak in the MR-AC, indicating a slight interaction additionally to the stronger interaction of the elution peak, fractionation and extended characterization of the peaks was performed. The peak tailing was more distinct for the high-mannose enriched mAbs obtained from the ConA product pool. Consequently, the peaks of the ConA product pools of three different mAbs (IgG1-A, IgG1-C, and ZweimAb-A) were fractionated. The flow-through peak was fractionated divided into three fractions (F1 “start”, F2 “middle”, F3 “end”) to isolate the peak tailing (F3), as well as the elution peak (F4) was fractionated (Figure 4a). Subsequently, the fractions were analyzed for intact mass using RPC-MS, showing that only symmetrical high-mannose glyco-pairs (M5/M5) were present in the elution peak (Figure S6). To further characterize the differences between symmetrical and asymmetrical high-mannose glyco-pairs, the fractions were digested with Endo F3. This enzyme cleaves all complex N-glycans, with core fucosylation, after the initial N-acetylglucosamine as described previously.⁴² Since

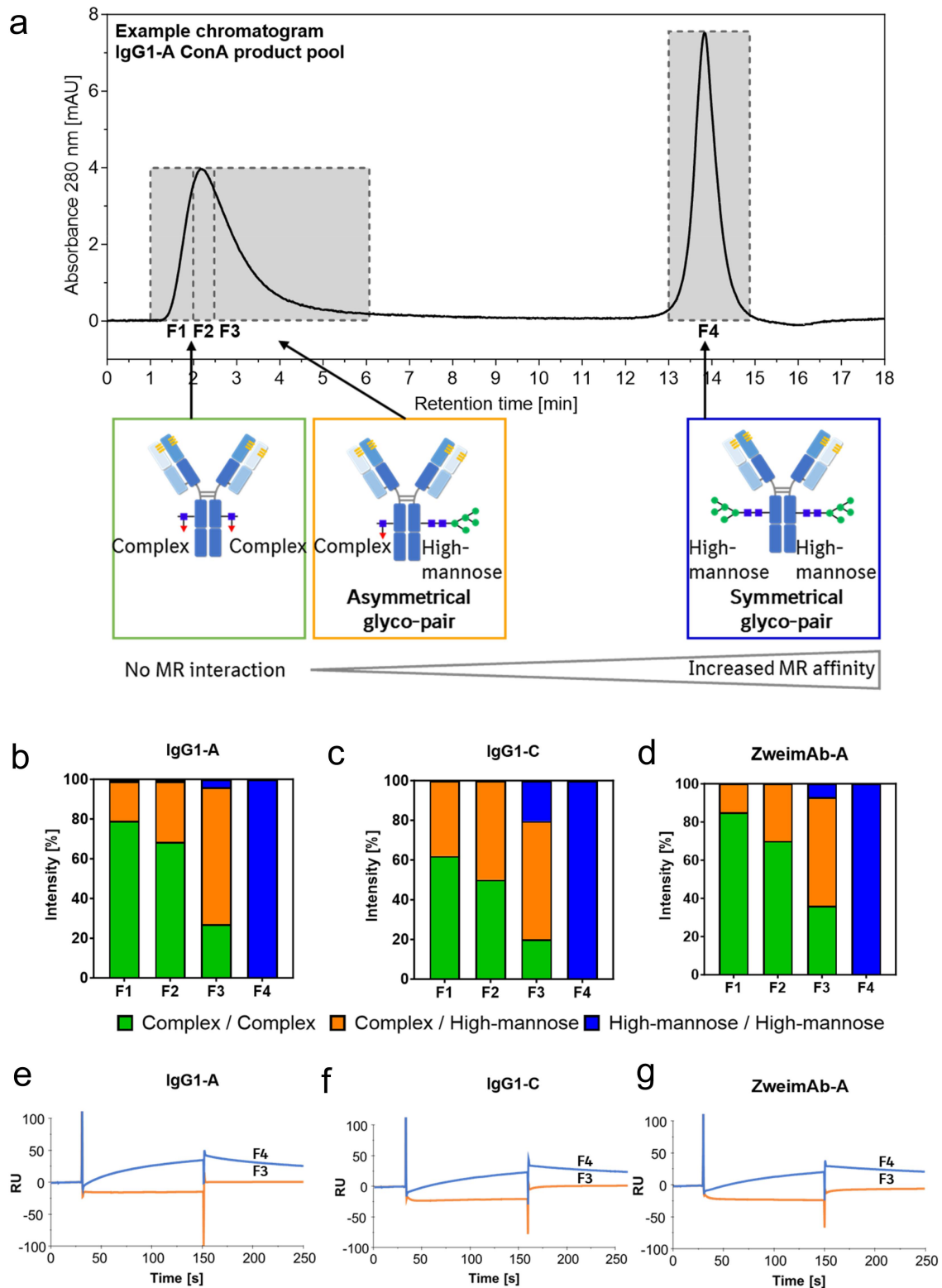


Figure 4. Evaluation of the asymmetrical and symmetrical high-mannose glyco-pair of mAbs regarding their MR interaction. The ConA product pools of three mAbs were analysed by MR-AC. The flow-through peak divided into three parts (F1-F3) and the elution peak (F4) were fractionated as illustrated (a). The fractions were analysed by RPC-MS after Endo F3 digestion leading to the distribution of the asymmetrical and symmetrical high-mannose glyco-pair in each fraction. Data is presented as the average of two MR-AC columns (b-d). The flow-through peak tailing (F3) and the elution peak (F4) were analysed by MR-SPR (e-g).

the mAbs mainly contain M5 high-mannose N-glycans, this digestion results in three different mAb glyco-pairs represented by three peaks in the intact mass spectra: 1) mAb with no mannose N-glycans due to prior glycosylation with only

complex fucosylated N-glycans, 2) mAb with one high-mannose N-glycan, and 3) mAb with two high-mannose N-glycans. Non-fucosylated N-glycans that are not cleaved by Endo F3 were not considered in the data analysis because

their abundance was marginal in all mAbs of this study. The Endo F3-digested samples were analyzed by RPC-MS, and the percentage intensity of each signal in the mass spectrum was determined relative to the other two signals, leading to the distribution of the three mAb glyco-pairs within one fraction (Figures 4b–d and S7). In this case, the elution peak (F4) contained the symmetrical high-mannose glyco-pairs for all three analyzed mAbs. By comparing the three fractions of the flow-through peak, an enrichment of the asymmetrical high-mannose glyco-pair from F1 to F3 toward the peak tailing was detected. Thus, the MR affinity column differentiates between the binding of different high-mannose glyco-pairs to the MR. The symmetrical high-mannose glyco-pair demonstrated the strongest MR binding, while the asymmetrical high-mannose glyco-pair showed the lowest. Characterization of the peak tailing (F3) and elution peak (F4) fractions by MR-SPR (Figure 4e–g) revealed a clear distinction between these fractions in the response signal height, showing a higher signal for F4 containing symmetrical high-mannose glyco-pair compared to F3 containing asymmetrical high-mannose glyco-pair, confirming the MR-AC results.

The ConA product pools of the mAbs leading to enriched high-mannose content were used to enhance the sensitivity of both the MR interaction and the intact mass spectra. The fractionation and characterization considering the glycan-pairing workflow was also applied to the reference mAb directly, exemplified by IgG1-A, to ensure that no bias was introduced from the ConA enrichment. The same different binding properties to the MR of the symmetrical and asymmetrical high-mannose glyco-pairs were determined (Figure S10). Thus, the observed effect is not attributable to the enriched high-mannose material leading to limited binding capacity of the column.

Due to the different MR binding affinity of the symmetrical and asymmetrical high-mannose glyco-pair, the elution peak area correlation was adapted to the Endo F3 symmetrical high-

mannose glyco-pair percentage (Figure 5a). This adjustment still reveals a linear relationship between the elution peak area and the percentage of the symmetrical high-mannose glyco-pair. Additionally, the degree of flow-through peak tailing was measured by determining the asymmetry at 30% peak height where the tailing was most prominent. This was then correlated with the percentage of Endo F3 asymmetrical high-mannose glyco-pair (Figure 5b). The results indicate that a higher degree of peak tailing, reflected in increased asymmetry, corresponds to a higher percentage of the asymmetrical high-mannose glyco-pair.

To investigate whether the flow-through peak tailing occurs due to high-mannose N-glycan of the asymmetrical glyco-pair or if there is a contribution of the complex N-glycan, IgG1-A was treated with Endo H. This enzyme specifically cleaves all high-mannose N-glycans, but no complex N-glycans.⁴² The cleavage was monitored using RPC-MS. The digested and undigested IgG1-A was analyzed by MR-SPR and MR-AC and involved the reference mAb and the ConA product pool (Figure S8). Upon comparing the results with the undigested material, the flow-through peak tailing and the elution peak were not determined for the Endo H-treated mAb. The digested mAb eluted in a flow-through peak, indicating no MR binding. Additionally, the MR-SPR sensorgrams showed a response signal for the undigested mAb, but none for the digested mAb.

Evaluation of the asymmetrical high-mannose glyco-pair of mAbs

As already observed in the intact mass spectra and after the Endo F3 digestion, mainly the asymmetrical high-mannose glyco-pairs of the mAbs were detected in the flow-through peak tailing (F3). To evaluate and relatively quantify these asymmetrical high-mannose glyco-pairs, an Endo H digestion of the fractions 1–4 for three different mAbs (IgG1-A, IgG1-C,

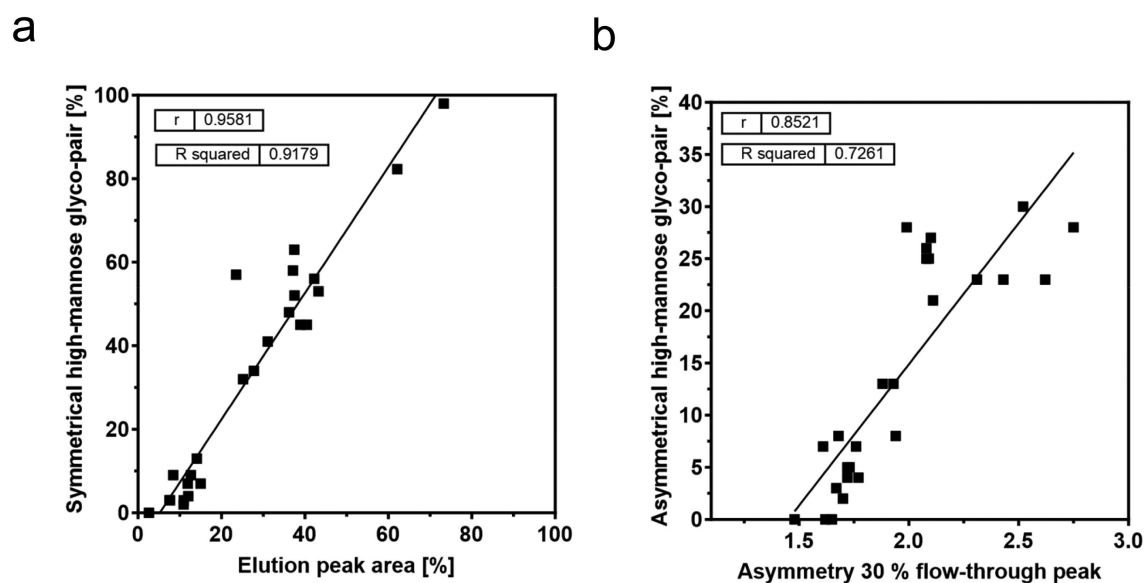


Figure 5. Correlations of the mAb screening by MR-AC. The elution peak area was correlated with the respective symmetrical high-mannose glyco-pair percentage (a). The asymmetry at the flow-through peak height of 30% was correlated with the respective asymmetrical high-mannose glyco-pair percentage (b). The percentage of the symmetrical or asymmetrical high-mannose glyco-pair of each mAb was determined by RPC-MS after Endo F3 digestion.

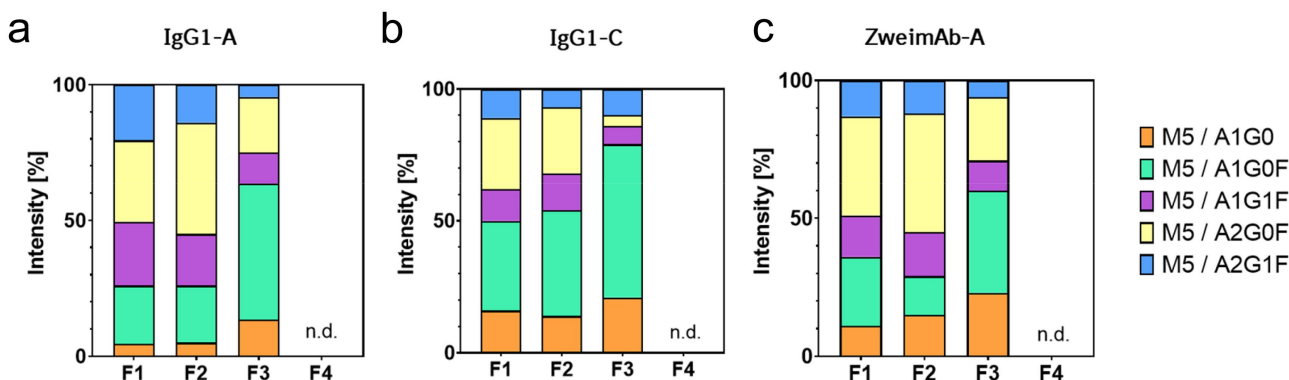


Figure 6. Determination of the complex N-glycan of the asymmetrical high-mannose glyco-pair and their distribution in the fractions of MR-AC analysis by RPC-MS after Endo H digestion. IgG1-A: data are presented as the average of two MR-AC columns, IgG1-C and ZweimAb-a: data are presented as the average of one MR-AC column, n.d. means not detected.

and ZweimAb-A) were performed and analyzed by RPC-MS. Endo H cleaves all high-mannose N-glycans after the initial N-acetylglucosamine, resulting in three distinct peak groups in the intact mass spectra: 1) the mAb peak of cleaved symmetrical high-mannose glyco-pairs, 2) the peak group with one cleaved high-mannose N-glycan, reflecting the asymmetrical high-mannose glyco-pair and 3) the peak group with two complex N-glycans containing mAbs. The second peak group facilitates the identification of the complex N-glycan of the asymmetrical glyco-pair. The intact mass spectra of the asymmetrical glyco-pair exhibited differences between the fractions of the flow-through peak (F1–3) of each mAb. The asymmetrical glyco-pair was not detected in the elution peak (F4) (Figure S9). To quantify these differences, the percentage intensity of each signal was calculated relative to the other signals in the mass spectrum for each mAb (Figure 6). For all three mAbs, the asymmetrical glyco-pair distribution at the “start” and “middle” of the flow-through peak (F1 and F2) was similar, but changed in F3, the flow-through peak tailing. In F3, the main asymmetrical glyco-pairs are the truncated, mono-antennary complex N-glycans lacking one N-acetylglucosamine, e.g., A1G0 and A1G0F, although the most common complex N-glycan is A2G0F (Figure 1).

Discussion

The MR is suggested to be responsible for the faster clearance rate of mAbs containing high-mannose N-glycans.^{2,13–17} To strengthen the hypothesis of the MR-mediated clearance mechanism, two methods were developed and applied to characterize the MR-mAb interaction: MR-SPR and MR-AC.

The MR-SPR method used physiological-like conditions. The method is similar to one reported previously.³⁹ Unlike Zhou *et al.*, who used only the CRD4-7 domains, both methods presented here use the full-length MR extracellular domain, allowing a more natural construct. The orthogonal method MR-AC enabled use of the full-length extracellular domain of the MR in the native state by mimicking the physiological conditions for binding. The bind/elute mode allowed quantification of the resolved peaks by their respective peak area or characterization by other peak features like asymmetry. Both methods were able to demonstrate the MR interaction with mAbs containing high-mannose N-glycans.

This was shown by an increased response signal of MR-SPR or elevated elution peak area of MR-AC compared to the Endo S-treated mAb, representing a deglycosylated mAb. The interaction of the MR with mAb material expressed with kifunensine, which leads to high mannose N-glycans ranging from M5-M9, was previously shown using MR-SPR.³⁹

An increase in the high-mannose content of mAbs corresponds to an elevation in the elution peak areas or response signals, indicating a dependency of the MR-mAb interaction on high-mannose N-glycans. The linear correlation between the high-mannose content of different mAbs and the elution peak area of MR-AC suggests that the MR directly interacts with the high-mannose N-glycans. Additionally, the MR-mAb interaction is not influenced by the length of the high-mannose N-glycan structure (M5-M9), as previously shown also for other molecules such as glucocerebrosidase.⁴³

The CRDs of the MR have affinity to terminal mannose, fucose, N-acetylglucosamine and slightly to galactose.⁷ Despite this, the linear correlation between high-mannose content and elution peak area suggests that there is no interaction with other complex N-glycans containing terminal N-acetylglucosamine or galactose of mAbs. This is further supported by the analysis of Endo H-treated samples, which cleaves high-mannose N-glycans, resulting in a mAb primarily composed of complex N-glycans. Compared to untreated samples, these treated samples exhibited no MR interaction neither in MR-AC nor MR-SPR. However, the reported affinity in literature could be attributed to glycoproteins with surface-exposed N-glycans. The mAb Fc γ can have two different conformations: the open conformation and the compact conformation. Thus, the high-mannose N-glycans may exhibit a more open conformation enabling MR interaction than complex N-glycans. Similar effects are shown for the Fc γ receptors.^{44,45}

To further confirm the binding of mAbs containing high-mannose N-glycans, the flow-through peak divided into three parts due to an asymmetrical peak shape and the elution peak of the MR-AC analysis were fractionated and characterized considering the glycan-pairing. The results revealed the binding of the symmetrical high-mannose glyco-pair to the MR and the asymmetrical glycoform was detected in the flow-through peak tailing, indicating a slight interaction with the MR. The study suggested an avidity effect. In current

glycoform-resolved PK studies the glycan pairing is neglected due to analysis of the released N-glycans by glycan map or on a peptide level.^{13–18,20} However, based on this MR-interaction study, the different binding affinity of the asymmetrical and symmetrical high-mannose glyco-pair to the MR could result in different clearance rates for each glyco-pair. Likely, only the symmetrical high-mannose glyco-pair of mAbs will be cleared faster compared to the asymmetrical high-mannose glyco-pair of mAbs or complex N-glycan containing mAbs. There can, however, be variations, as the PK study reported by Goetze *et al.* lead to the assumption that a single M5 N-glycan per mAb is sufficient to increase clearance mediated by the MR.¹⁶ Another PK study reported recently, implies that the clearance rates in humans for mAbs containing high-mannose are comparable, irrespective of the asymmetrical or symmetrical pairing.³⁴ Herein the detected slight interaction of the asymmetrical glyco-pair may indeed be sufficient for MR binding, but further investigation is needed. Currently, the application of MR-AC is designed solely for the purpose of thorough characterization and not for PK prediction. The dimensions of the MR-AC column are not optimal for the separation of the asymmetrical glyco-pair. It could be possible that, with a longer column and lower flow rate, the resolution will be increased and the peak tailing could be resolved into a separate peak. The potential differences in the clearances rates due to the avidity effect of the symmetrical high-mannose glyco-pair to MR need to be proven in a glyco-pair-resolved PK study. If the avidity effect of the symmetrical high-mannose glyco-pair is shown *in vivo*, an adjustment of the criticality with respect to PK of high-mannose N-glycans in CQA assessments will be necessary. This will affect the analytical strategy of N-glycans, which is currently based on glycan maps, but usually does not encompass the glycan-pairing.

Furthermore, this avidity effect is suggested to be specific to mAbs. The control molecule RNase B binds to the MR, which has one N-glycosylation site⁴⁰ with mainly M5 and M6 N-glycans. Other examples are TPA and ovalbumin. TPA has various N-glycosylation sites, including one with high-mannose N-glycans, and ovalbumin has one N-glycosylation site with high-mannose N-glycans. It has been demonstrated that TPA and ovalbumin can bind to the MR, resulting in faster clearance.^{3,6} The control molecule RNase B further showed differences in the binding affinities compared to mAbs. This is probably due to different surface exposure of the high-mannose glycans of various glycoproteins leading to different MR accessibility.

Using MR-SPR, the binding affinities of various mAb formats or sequence variants in the Fc-region, such as the ZweimAb knob-into-hole structure, were compared, but no effects were noticeable. The highly conserved C_H2 domain contributes to the similar apparent binding affinities in the single-digit μ M range. Differentiating and comparing the binding affinities using a mixture of molecules with varying asymmetrical and symmetrical high-mannose mAb content is challenging. To observe differences in the apparent binding affinities, it may be necessary to normalize on the symmetrical high-mannose mAb content rather than solely on high-mannose content or protein concentration.

The slight MR interaction of the asymmetrical high-mannose glyco-pair in the flow-through peak tailing

prompted further investigation. Despite their low abundance, M5 was primarily paired with truncated or monoantennary N-glycans lacking N-acetylglucosamine. This is contrary to expectations, as A2G0F, due to its prevalence in mAbs, is typically anticipated to be the predominant pairing partner. Falck *et al.* recently reported two recent PK studies that showed high-mannose and truncated monoantennary N-glycans clear more rapidly than complex N-glycans, but high-mannose N-glycans displayed the fastest clearance.^{14,15} The effect of the faster clearance of truncated N-glycans is likely not increased by the removal of the second N-acetylglucosamine. This could indicate that exposed core mannoses do not strongly increase clearance compared to outer arm mannoses. Furthermore, the pairing of M5 primarily with monoantennary complex N-glycans and its slight interaction with the MR could account for the increased clearance for different monoantennary complex N-glycans observed by Falck *et al.* The flow-through peak tailing suggests that monoantennary complex N-glycans contribute minimally, if at all, to the MR binding. This tailing disappears after the high-mannose N-glycans are cleaved by Endo H, likely due to a minor interaction of the M5 pairing partner with the MR rather than the affinity from the core mannoses or the N-acetylglucosamine to the MR. Furthermore, recent PK profiles showing the N-glycan distribution over time after administration exhibit a biphasic PK profile for M5 N-glycans meaning the clearance rate varies over time.^{13,17} The M5 N-glycans decrease and then a plateau tends to set up. Higel *et al.* previously reported the incomplete removal of the M5 N-glycans from circulation indicating different mechanisms for different glyco-pairs.¹⁷ This could be correlated to possible different clearance rates of asymmetrical or symmetrical high-mannose glyco-pairs showing different MR binding affinities. The strong alignment between MR-mAb interactions and the recent PK studies reinforces the hypothesis of the MR role in the clearance mechanism of mAbs with high-mannose or monoantennary N-glycans.

In conclusion, this study systematically demonstrated the MR-mAb interaction by applying two novel methods, MR-SPR and MR-AC. The findings enhance the understanding of the MR-mAb interaction and reinforce the theory of MR-mediated clearance mechanism. The data indicate that the interaction of MR with the Fc region of mAbs is dependent on high-mannose type N-glycan presence, but not on the length of the high-mannose structure (M5–M9). No interaction was observed with other complex N-glycans that contain terminal N-acetylglucosamine or galactose. Furthermore, the interaction is not influenced by the sequence and mAb format, including IgG1 and IgG4, and bispecific formats with substitutions for the knob-into-hole construct and/or effector function silencing. A key finding was the stronger binding of the symmetrical high-mannose glyco-pair to the MR compared to the asymmetrical high-mannose glyco-pair, suggesting an avidity effect that could result in differing clearance rates for each glyco-pair, which has also been seen in published PK studies. Further investigations such as glyco-pair resolved PK studies are needed. This study could serve as a valuable guide for potential cell-based and *in vivo* PK studies. The study also revealed that M5 was primarily paired with monoantennary

N-glycans, indicating that exposed core mannoses do not strongly interact with MR compared to outer arms mannose residues and the pairing with high-mannose N-glycans could explain the faster clearance of these monoantennary N-glycans.

In summary, the presented data are in good agreement with previously published N-glycan PK data and supports the hypothesis of the MR being responsible for the increased clearance of glycoproteins containing high-mannose type N-glycans.

Material and methods

Proteins

RNAse B was purchased from New England Biolabs. BSA was from Merck. The different mAbs were produced by mammalian cell culture technology using a CHO cell line and afterwards purified and formulated. The mAbs are either IgG1 / 4 or formatted as ZweimAb or DoppelmAb as described previously.⁴¹

Preparation of mAbs with different high-mannose content

mAbs enriched in high-mannose content were achieved by ConA chromatography. A 5 mL HiTrapTM ConA 4B column (Cytiva) was used on a ÄktaTM go system (Cytiva) at room temperature, following the manufacturer's protocol. Data acquisition and instrument control were performed by Unicorn (version 7.5., Cytiva). The column was loaded with 10 mg mAb and eluted by 0.2 M methyl- α -D-glucopyranoside. A flow rate of 5 mL/min was used except for binding and elution, which was performed at 1 mL/min. The product pool was collected, concentrated and analyzed by glycan map and RPC-MS.

Kifunensine, a mannosidase inhibitor, was used in cell culture as previously described,^{20,39} to generate mAbs with mainly high-mannose N-glycans. An inhibitor concentration of 100 ng/mL was used. The material was purified by Protein A chromatography and formulated, and subsequently analyzed by glycan map and RPC-MS.

Enzyme digestions

Three different enzymes from New England Biolabs were used to change the N-glycan compositions of the mAbs. For 100 μ g mAb 4 μ L of Endo S were used in 1X GlycoBuffer 1 with a final volume of 20 μ L. After incubation of 1 h at 37°C, the reaction was controlled by RPC-MS and HILIC.

For 10 μ g mAb 1 μ L Endo F3 were used in 1X GlycoBuffer 4 in a final volume of 20 μ L. For 10 μ g mAb, 5 μ L Endo H were used in 1X GlycoBuffer 3 in a final volume of 20 μ L. Endo F3 and Endo H digestions were incubated overnight at 37°C and controlled by RPC-MS.

For 100 μ g mAb, 16 μ L of α -1,2-mannosidase from *Aspergillus saitoi* (25 mU/mL, Agilent Technologies) were used in 100 mM sodium acetate, 0.5 mM CaCl₂, pH 5.0 with a final volume of 30 μ L. After incubation for >72 h at 37°C, the digestion was controlled by RPC-MS, as previously described.²⁰

Characterization of samples and fractions

Glycan map: determination of 2-AA labeled N-glycans composition by RPC

After buffer exchange to 1X phosphate-buffered saline (PBS) of 50 μ g sample, 1.5 μ L Rapid PNGase F were added to release the N-glycans of the mAbs followed by incubation for 30 min at 50°C. Subsequently, 40 μ L of labeling solution (0.73 M 2-AA (2-anthranilic acid), 0.75 M 2-methylpyridine borane complex in 85:15 ethanol:acid mixture) was added. Labeling of N-glycans was carried out for 2 h at 65°C. In order to remove the reaction mixture, the solution was evaporated until completely dry using a vacuum concentrator. N-glycans were reconstituted with 40 μ L water. For purification of the N-glycans from excess label and by-products of the reductive amination, 35 μ L were diluted with 400 μ L acetonitrile and loaded onto PhyTip[®] HILIC columns. Previously, the PhyTips[®] HILIC columns were pre-conditioned with water and acetonitrile. After three washing steps with 96% (v/v) acetonitrile containing 2% (v/v) formic acid, the N-glycans were eluted with two times 100 μ L water. The purified N-glycan solution was heated for an additional 30 min at 50°C to remove any remaining acetonitrile.

N-glycans were separated using RPC as previously described.⁴⁶ The chromatographic separation was performed on Zorbax RRHD Bonus-RP column (2.1 \times 150 mm, 1.8 μ m, 80 Å, Agilent) using a 1290 Infinity II UHPLC system (Agilent). RPC was operated at a flow rate of 0.250 mL/min and a column temperature of 70°C. The mobile phases consisted of water with 0.5% acetic acid and 0.5% formic acid (A) and of water with 20% acetonitrile, 5% 1-propanol, 5% 1-butanol, 0.5% acetic acid, and 0.5% formic acid (B). The following linear gradient was applied 0.00:2, 33.00:35, 48.00:95, 53.00:95, 54.00:2, 59.00:2 (time in min:percentage of mobile phase B). Fluorescence detection of 2-AA-labeled N-glycans was carried out with an excitation wavelength of 350 nm and emission wavelength of 440 nm.

Intact mass analysis of mAbs by RPC-MS

A BioAccord LC-MS system (Waters) consisting of an ACQUITY UPLC I-Class PLUS system and an electrospray ionization – time of flight (ESI-ToF)-based ACQUITY RDa detector was used and controlled by UNIFI Scientific Information Software (Waters). The MS data were collected in positive ionization mode. RPC was performed on a BioResolve Reverse Phase mAb Polyphenyl Column (450 Å, 2.7 μ m, 2.1 \times 50 mm, Waters) equilibrated at 80°C and operated at a flow rate of 0.25 mL/min. Mobile phase A was 0.1% formic acid in water and mobile phase B was 0.09% formic acid in 2-propanol. 2 μ g sample were injected and analyzed with the following gradient: 0.00:15, 1.00:15, 9.00:35, 9.20:95, 10.20:95, 10.40:15, 13.00:15 (time in min:percentage of mobile phase B). Elution was monitored at 214 nm. In full scan mode, MS data were acquired within a mass range of 400–7000 m/z at positive polarity, employing a 2 Hz scan rate, 140 V cone voltage, and standard lockmass correction mode. The capillary voltage was adjusted to 1.5 kV, the desolvation temperature was set to 550°C. Data analysis was

conducted using the UNIFI Scientific Information System, which used the MaxEnt1 deconvolution algorithm.

HILIC for deglycosylation efficiency

For sample preparation, a denaturation buffer consisting of 6.0 M guanidine-HCl, 50 mM Tris-HCl and 5 mM EDTA, as well as a 5 mg/mL Tris(2-carboxyethyl)phosphine (TCEP) solution in 1X PBS was prepared. After buffer exchange of the samples to 1X PBS, 100 µg of deglycosylated mAb and of the control mAb were denatured by addition of the denaturing buffer at 12.5 µL per 100 µL sample. The sample was incubated for 15 min at 70°C and 1300 rpm.

For the analysis, 0.5 µL of the sample were injected onto the Waters ACQUITY UPLC Glycoprotein (2.1 × 150 mm, 1.7 µm, 300 Å) column. The chromatographic separation was performed on a 1290 Infinity II UHPLC system (Agilent). HILIC was operated at a flow rate of 0.450 mL/min and a temperature of 80°C. The mobile phases consisted of water with 0.1% trifluoroacetic acid (A) and acetonitrile with 0.1% trifluoroacetic acid (B). The following linear gradient was applied 0.00:85, 0.20:72, 10.20:64, 11.00:10, 20.00:10, 21.00:85, 25.00:85 (time in min:percentage of mobile phase B). Elution was monitored at 214 nm.

Cloning, expression and purification of human MR

The full extracellular domain of the human MR C-type 1 with a C-terminal histidine tag and Biotin AviTag was cloned into an expression vector. The MR was transiently expressed in HEK-F cells. Just prior to transfection, HEK-F cells were transferred with a cell density of 2.0×10^6 cells/mL and > 99% cell viability into three 5 L shake flasks containing 2.2 L of Free Style F17 medium (Invitrogen) with 6 mM L-glutamine and 0.1% Pluronic F68 in each flask. HEK-F cells were transfected using polyethylenimine-mediated transfection method. Cells were incubated at 37°C with 5% CO₂ and 110 rpm after transfection. Twenty-four-hour post transfection, 2% Cytiva Cell boost™, 0.02% Cytiva Cell boost™ 7b and 2 g/L glucose were added. Forty-eight-hour post transfection, 3 mM Valproic acid was added and the temperature was shifted from 37°C to 33°C. One hundred and twenty-hour post transfection 1% Cytiva Cell boost™, 0.01% Cytiva Cell boost™ 7b were added. The supernatant was harvested 144 h post-transfection and clarified using 0.22 µm membrane filter.

For purification a Ni-NTA affinity chromatography was used as first step, followed by size exclusion chromatography (SEC) using the formulation buffer of 20 mM HEPES, 100 mM NaCl, 40 mM arginine, 0.01% CHAPS, pH 7.2. Purified MR was quantified using a NanoDrop spectrophotometer and analyzed by SDS PAGE and analytical SEC.

Affinity column preparation

After washing 1 mL Streptavidin Sepharose High Performance resin (Cytiva) with packing buffer (10 mM HEPES, 140 mM NaCl, 2.5 mM CaCl₂, pH 7.4) 6 mg of MR were added and incubated for 2 h with shaking. The coupling reaction was confirmed by RPC. The receptor

coupled beads were filled in a 5/50 Tricorn column (Cytiva). Equilibration of the MR affinity column was performed with 12 mM Tris, 140 mM NaCl, 2.5 mM CaCl₂, pH 7.4 and column efficiency was tested by injection of 10 µL 1 M NaCl.

Mannose receptor affinity chromatography

The ~1 mL MR affinity column (0.5 × ~5.0 cm) was used on a Äkta™ go system (Cytiva) at room temperature. Data acquisition and instrument control were performed by Unicorn (version 7.5., Cytiva). The column was equilibrated with mobile phase A (12 mM Tris, 140 mM NaCl, 2.5 mM CaCl₂, pH 7.4) followed by injection of 20 µg sample. Subsequently, a 12 min gradient from 0% to 100% mobile phase B (12 mM Tris, 140 mM NaCl, 20 mM EDTA, pH 7.4) was conducted, followed by 5 min at 100% mobile phase B. Re-equilibration was performed with mobile phase A after each run. During analysis, flow rate was kept at 0.50 mL/min and elution was detected via UV at 280 nm. Fraction collection was conducted with the Cytiva Fraction Collector F9-R. To obtain sufficient amounts of protein, fractions of different chromatographic runs were collected, pooled and concentrated. Samples were buffer exchanged to mobile phase A. The column was stored at 2–8°C in 10 mM acetate, 140 mM NaCl, 0.01 mg/mL PS20, 0.05% ProClin3000, pH 5.0 and a protease inhibitor mixture (cOmplete ULTRA) was added (1 tablet/50 mL).

Mannose receptor surface plasmon resonance analysis

A Biacore T200 instrument (Cytiva) and a flow cell referenced method was used. The MR was captured onto immobilized neutravidin on a sensor chip CM5 (Cytiva) to a level of 800–1000 response units (RU). Neutravidin was immobilized on the reference flow cell. All interaction analyses were performed at 25°C at a flow rate of 10 µL/min with 10 mM HEPES, 140 mM NaCl, 2.5 mM CaCl₂, 0.05% Tween20, pH 7.4 as running buffer using mild regeneration (10 mM HEPES pH 7.4, 140 mM NaCl, 20 mM EDTA or 10 mM HEPES pH 5.8, 140 mM NaCl). All samples were prepared by buffer exchange into the running buffer. Experiments were processed and analyzed in Biacore T200 Evaluation Software version 3.0. For the relative binding analysis, the mAbs variants were diluted to a concentration of 1 µM and measured with an association time of 120 s and a dissociation time of 120 s. For kinetic analyses, the samples were prepared as a 3-fold dilution series from 15 µM with an association time of 180 s and a dissociation time of 360 s. Kinetic data were double referenced and fitted globally to a steady state affinity.

Acknowledgments

The authors would like to thank Jörg Thomas Regula for comments and suggestions.

Disclosure statement

Julia Baumeister, Maximilian Meudt, Michaela Blech and Fabian Higel are employees of Boehringer Ingelheim GmbH & Co. KG, which is developing, manufacturing, and marketing biopharmaceutical products.

Kristina Aertker was an employee of Boehringer Ingelheim GmbH & Co. KG, when this study was conducted.

References

- Liu L. Pharmacokinetics of monoclonal antibodies and Fc-fusion proteins. *Protein Cell*. 2018;9(1):15–32. doi:10.1007/s13238-017-0408-4.
- Wright BA, Morrison SL. Effect of altered Ca²⁺-associated carbohydrate structure on the functional properties and in vivo fate of chimeric mouse-human immunoglobulin G1. *J Exp Med*. 1994;180(3):1087–1096. doi:10.1084/jem.180.3.1087.
- Grete M, Magnusson S, Berg T, Smedsrød B. Receptor-mediated endocytosis of ovalbumin by two carbohydrate-specific receptors in rat liver cells. *Biochemical J*. 1990;270(1):197–203. doi:10.1042/bj2700197.
- Kogelberg H, Tolner B, Sharma SK, Lowdell MW, Qureshi U, Robson M, Hillyer T, Pedley RB, Verweken W, Contreras R, et al. Clearance mechanism of a mannose-6-phosphate-enzyme fusion protein used in experimental cancer therapy. *Glycobiology*. 2006;17(1):36–45. doi:10.1093/glycob/cwl053.
- Lee SJ, Evers S, Roeder T, Parlow AF, Risteli J, Risteli L, Lee YC, Feizi T, Langen H, Nussenzweig MC, et al. Mannose receptor-mediated regulation of serum glycoprotein homeostasis. *Science*. 2002;295(5561):1898–901. doi:10.1126/science.1069540.
- Smedsrød B, Einarsson M, Pertoft H. Tissue plasminogen activator is endocytosed by mannose and galactose receptors of rat liver cells. *Thromb Haemostasis*. 1988;59(3):480–484. doi:10.1055/s-0038-1647519.
- Allavena P, Chieppa M, Monti P, Piemonti L. From pattern recognition receptor to regulator of homeostasis: the double-faced macrophage mannose receptor. *Crit Rev Immunol*. 2004;24(3):179–192. doi:10.1615/CritRevImmunol.v24.i3.20.
- Feinberg H, Jégouzo SAF, Lasanajak Y, Smith DF, Drickamer K, Weis WI, Taylor ME. Structural analysis of carbohydrate binding by the macrophage mannose receptor CD206. *J Biol Chem*. 2021;296(22):100368. doi:10.1016/j.jbc.2021.100368.
- Taylor PR, Gordon S, Martinez-Pomares L. The mannose receptor: linking homeostasis and immunity through sugar recognition. *Trends Immunol*. 2005;26(2):104–110. doi:10.1016/j.it.2004.12.001.
- East L, Isacke CM. The mannose receptor family. *Biochim et Biophys Acta (BBA) - Gen Subj*. 2002;1572(2–3):364–386. doi:10.1016/S0304-4165(02)00319-7.
- Taylor ME, Bezoulka K, Drickamers K. Contribution to ligand binding by multiple carbohydrate-recognition domains in the macrophage mannose receptor*. *J Biol Chem*. 1992;267(3):1719–1726. doi:10.1016/S0021-9258(18)46005-X.
- Taylor ME, Drickamer K. Structural requirements for high affinity binding of complex ligands by the macrophage mannose receptor. *J Biol Chem*. 1993;268(1):399–404. doi:10.1016/s0021-9258(18)54164-8.
- Alessandri L, Ouellette D, Acquah A, Rieser M, LeBlond D, Saltarelli M, Radziejewski C, Fujimori T, Correia I. Increased serum clearance of oligomannose species present on a human IgG1 molecule. *mAbs*. 2012;4(4):509–520. doi:10.4161/mabs.20450.
- Falck D, Thomann M, Lechmann M, Koeleman CAM, Malik S, Jany C, Wuhrer M, Reusch D. Glycoform-resolved pharmacokinetic studies in a rat model employing glycoengineered variants of a therapeutic monoclonal antibody. *mAbs*. 2021;13(1). doi:10.1080/19420862.2020.1865596.
- Falck D, Lechmann M, Momčilović A, Thomann M, Koeleman CAM, Jany C, Malik S, Wuhrer M, Reusch D. Clearance of therapeutic antibody glycoforms after subcutaneous and intravenous injection in a porcine model. *mAbs*. 2022;14(1). doi:10.1080/19420862.2022.2145929.
- Goetze AM, Liu YD, Zhang Z, Shah B, Lee E, Bondarenko PV, Flynn GC. High-mannose glycans on the Fc region of therapeutic IgG antibodies increase serum clearance in humans. *Glycobiology*. 2011;21(7):949–959. doi:10.1093/glycob/cwr027.
- Higel F, Seidl A, Demelbauer U, Viertlboeck-Schudy M, Koppenburg V, Kronthaler U, Sörgel F, Frieß W. N-glycan PK profiling using a high sensitivity nanoLCMS work-flow with heavy stable isotope labeled internal standard and application to a preclinical study of an IgG1 biopharmaceutical. *Pharm Res*. 2015;32(11):3649–3659. doi:10.1007/s11095-015-1724-0.
- Kanda Y, Yamada T, Mori K, Okazaki A, Inoue M, Kitajima-Miyama K, Kuni-Kamochi R, Nakano R, Yano K, Kakita S, et al. Comparison of biological activity among nonfucosylated therapeutic IgG1 antibodies with three different N-linked Fc oligosaccharides: the high-mannose, hybrid, and complex types. *Glycobiology*. 2007;17(1):104–118. doi:10.1093/glycob/cwl057.
- Chen X, Liu D, Flynn GC. The effect of Fc glycan forms on human IgG2 antibody clearance in humans. *Glycobiology*. 2009;19(3):240–249. doi:10.1093/glycob/cwn120.
- Yu M, Brown D, Reed C, Chung S, Lutman J, Stefanich E, Wong A, Stephan J-P, Bayer R. Production, characterization and pharmacokinetic properties of antibodies with N-linked mannose-5 glycans. *mAbs*. 2017;4(4):475–487. <https://teach.com/blog/six-snapchat-projects-for-a-classroom/>.
- Roopenian DC, Akilesh S. FcRn: the neonatal Fc receptor comes of age. *Nat Rev Immunol*. 2007;7(9):715–725. doi:10.1038/nri2155.
- Dashivets T, Thomann M, Rueger P, Knaupp A, Buchner J, Schlothauer T. Multi-angle effector function analysis of human monoclonal IgG glycovariants. *PLOS ONE*. 2015;10(12):1–24. doi:10.1371/journal.pone.0143520.
- Gahaur J, Heidenreich A-K, Somsen GW, Bulau P, Reusch D, Wuhrer M, Habberger M. Detailed characterization of monoclonal antibody receptor interaction using affinity liquid chromatography hyphenated to native mass spectrometry. *Analytical Chem*. 2017;89(10):5404–5412. doi:10.1021/acs.analchem.7b00211.
- Wada R, Matsui M, Kawasaki N. Influence of N-glycosylation on effector functions and thermal stability of glycoengineered IgG1 monoclonal antibody with homogeneous glycoforms. *mAbs*. 2019;11(2):350–372. doi:10.1080/19420862.2018.1551044.
- Wang W, Vlasak J, Li Y, Pristatsky P, Fang Y, Pittman T, Roman J, Wang Y, Prueksaritanont T, Ionescu R, et al. Impact of methionine oxidation in human IgG1 Fc on serum half-life of monoclonal antibodies. *Mol Immunol*. 2011;48(6–7):860–866. doi:10.1016/j.molimm.2010.12.009.
- Jefferis R. Glycosylation as a strategy to improve antibody-based therapeutics. *Nat Rev Drug Discov*. 2009;8(3):226–234. doi:10.1038/nrd2804.
- Reusch D, Tejada ML. Fc glycans of therapeutic antibodies as critical quality attributes. *Glycobiology*. 2015;25(12):1325–1334. doi:10.1093/glycob/cwv065.
- Zhou Q, Qiu H. The mechanistic impact of N-Glycosylation on stability, pharmacokinetics, and immunogenicity of therapeutic proteins. *J Pharm Sci*. 2019;108(4):1366–1377. doi:10.1016/j.xphs.2018.11.029.
- Higel F, Seidl A, Sörgel F, Friess W. N-glycosylation heterogeneity and the influence on structure, function and pharmacokinetics of monoclonal antibodies and Fc fusion proteins. *Eur J Pharm Biopharmaceutics*. 2016;100:94–100. doi:10.1016/j.ejpb.2016.01.005.
- Luo S, Zhang B. Benchmark glycan profile of therapeutic monoclonal antibodies produced by mammalian cell expression systems. *Pharm Res [Prepr]*. 2023;41(1):29–37. doi:10.1007/s11095-023-03628-4.
- Mastrangeli R, Audino MC, Palinsky W, Broly H, Bierau H. The formidable challenge of controlling high mannose-type N-Glycans in therapeutic mAbs. *Trends Biotechnol*. 2020;38(10):1154–1168. doi:10.1016/j.tibtech.2020.05.009.
- Tharmalingam T, Wu C-H, Callahan S, Goudar CT. A framework for real-time glycosylation monitoring (RT-GM) in mammalian cell culture. *Biotechnol Bioeng*. 2015;112(6):1146–1154. doi:10.1002/bit.25520.

33. Zupke C, Brady LJ, Slade PG, Clark P, Caspary RG, Livingston B, Taylor L, Bigham K, Morris AE, Bailey RW, et al. Real-time product attribute control to manufacture antibodies with defined N-linked glycan levels. *Biotechnol Prog.* 2015;31(5):1433–1441. doi:10.1002/btpr.2136.
34. Liu YD, Flynn GC. Biologicals effect of high mannose glycan pairing on IgG antibody clearance. *Biologicals.* 2016;44(3):163–169. doi:10.1016/j.biologicals.2016.02.003.
35. Andersen CBF, Moestrup SK. How calcium makes endocytic receptors attractive. *Trends Biochemical Sci.* 2014;39(2):82–90. doi:10.1016/j.tibs.2013.12.003.
36. Gazi U, Martinez-Pomares L. Influence of the mannose receptor in host immune responses. *Immunobiology.* 2009;214(7):554–561. doi:10.1016/j.imbio.2008.11.004.
37. Hu Z, Shi X, Yu B, Li N, Huang Y, He Y. Structural insights into the pH-dependent conformational change and collagen recognition of the human mannose receptor. *Structure.* 2018;26(1):60–71. e3. doi:10.1016/j.str.2017.11.006.
38. Kim J, Albarghouthi M. Rapid monitoring of high-mannose glycans during cell culture process of therapeutic monoclonal antibodies using lectin affinity chromatography. *J Sep Sci.* 2022; (December 2021):1–9. doi:10.1002/jssc.202100903.
39. Zhou Q, Shankara S, Roy A, Qiu H, Estes S, McVie-Wylie A, Culm-Merdek K, Park A, Pan C, Edmunds T, et al. Development of a simple and rapid method for producing non-fucosylated oligo-mannose containing antibodies with increased effector function. *Biotechnol Bioeng.* 2008;99(3):652–665. doi:10.1002/bit.21598.
40. Rudd PM, Joao HC, Coghill E, Fiten P, Saunders MR, Opendakker G, Dwek RA. Glycoforms modify the dynamic stability and functional activity of an enzyme. *Biochemistry.* 1994;33(1):17–22. doi:10.1021/bi00167a003.
41. Venkataramani S, Low S, Weigle B, Dutcher D, Jerath K, Menzenski M, Frego L, Truncali K, Gupta P, Kroe-Barrett R, et al. Design and characterization of Zweimab and Doppelmab, high affinity dual antagonistic anti-TSLP/IL13 bispecific antibodies. *Biochem Biophys Res Commun.* 2018;504(1):19–24. doi:10.1016/j.bbrc.2018.08.064.
42. Meudt M, Baumeister J, Mizaikoff B, Ebert S, Rosenau F, Blech M, Higel F. Comprehensive analysis and characterization of glycan pairing in therapeutic antibodies and Fc-containing biotherapeutics: addressing current limitations and implications for N-glycan impact. *Eur J Pharm Biopharmaceutics.* 2024;200:114325. doi:10.1016/j.ejpb.2024.114325.
43. Van Patten SM, Hughes H, Huff MR, Piepenhagen PA, Waire J, Qiu H, Ganesa C, Reczek D, Ward PV, Kutzko JP, et al. Effect of mannose chain length on targeting of glucocerebrosidase for enzyme replacement therapy of gaucher disease. *Glycobiology.* 2007;17(5):467–478. doi:10.1093/glycob/cwm008.
44. Borrok MJ, Jung ST, Kang TH, Monzingo AF, Georgiou G. Revisiting the role of glycosylation in the structure of human IgG Fc. *ACS Chem Biol.* 2012;7(9):1596–1602. doi:10.1021/cb300130k.
45. Chen CL, Hsu J-C, Lin C-W, Wang C-H, Tsai M-H, Wu C-Y, Wong C-H, Ma C. Crystal structure of a homogeneous IgG-Fc glycoform with the N-Glycan designed to maximize the antibody dependent cellular cytotoxicity. *ACS Chem Biol.* 2017;12(5):1335–1345. doi:10.1021/acscchembio.7b00140.
46. Wilhelm JG, Dehling M, Higel F. High-selectivity profiling of released and labeled N-glycans via polar-embedded reversed-phase chromatography. *Analytical Bioanal Chem.* 2019;411(3):735–743. doi:10.1007/s00216-018-1495-7.